

Nonequilibrium Quantum Dynamics of a Charge Carrier Doped into a Mott Insulator

M. Mierzejewski,^{1,2} L. Vidmar,² J. Bonča,^{2,3} and P. Prelovšek^{2,3}

¹*Institute of Physics, University of Silesia, 40-007 Katowice, Poland*

²*J. Stefan Institute, SI-1000 Ljubljana, Slovenia*

³*Department of Physics, FMF, University of Ljubljana, Jadranska 19, SI-1000 Ljubljana, Slovenia*

(Received 18 February 2011; published 9 May 2011)

We study real-time dynamics of a charge carrier introduced into an undoped Mott insulator propagating under a constant electric field F on the t - J ladder and a square lattice. We calculate the quasistationary current. In both systems an adiabatic regime is observed followed by a positive differential resistivity (PDR) at moderate fields where the carrier mobility is determined. Quantitative differences between the ladder and two-dimensional (2D) systems emerge when at large fields both systems enter the negative differential resistivity (NDR) regime. In the ladder system Bloch-like oscillations prevail, while in two dimensions the current remains finite, proportional to $1/F$. The crossover between the PDR and NDR in two dimensions is accompanied by a change of the spatial structure of the propagating spin polaron.

DOI: 10.1103/PhysRevLett.106.196401

PACS numbers: 71.27.+a, 72.10.Bg

Introduction.—The real-time response of interacting many-body quantum systems remains in many aspects an unexplored field that has recently attracted significant attention. Understanding of the time-dependent phenomena becomes vital for various branches of physics including condensed matter [1], nanostructures [2] and optical lattice systems [3,4]. Since only very few cases are exactly solvable, the vast majority of unbiased results has been obtained from numerical approaches like exact diagonalization (ED) [5,6], time-dependent density matrix renormalization group [7] or nonequilibrium dynamical mean-field theory [8]. Among others, the electric-field induced breakdown of the Mott insulator (MI) [5,9–11], nonequilibrium transport in nanostructures [12,13] and the relaxation of correlated systems after the photoexcitations [14,15], represent the well-studied examples of nonequilibrium phenomena which are important both for fundamental understanding of strongly correlated systems as well as for their potential applications.

Most of theoretical studies so far considered the breakdown of *undoped* MI, when the threshold value of the electric field exceeds experimental value [9] by a few orders of magnitude (see discussion in Ref. [11]). It indicates that other transport mechanism becomes active at energies much lower than the Mott-Hubbard gap. In this Letter we investigate a nonequilibrium response of a charge carrier doped into the insulator and driven by a uniform electric field F . Understanding of this subject on one hand widens our knowledge of a charge carrier doped into the antiferromagnetic (AFM) background [16,17], on the other, it represents a fundamental problem of a quantum particle moving in a dissipative medium [18].

Having in mind strongly correlated systems, we investigate the t - J model where the particle driven by a constant electric field dissipates the energy by inelastic scattering on spin degrees of freedom. We use numerical approaches to

treat the t - J model at zero temperature on two different system geometries, i.e., a ladder with periodic boundary conditions and an infinite two-dimensional (2D) square lattice.

The most important finding of this Letter concerns the current-field characteristic, where the linear part with a well-defined mobility is followed by a strongly nonlinear one with a negative differential resistivity. Numerical results reveal also adiabatic evolution for very weak fields (below the linear regime) and strong Bloch oscillations (BO) in the opposite limit of large F . These qualitative results hold for both the geometries. The most prominent difference between the ladder and the 2D case emerges at large field where in the latter system due to different topology, allowing for transverse charge carrier motion, BO remain damped and the steady current decreases with field as $1/F$.

Model.—We consider a charge carrier within the t - J model threaded by a time-dependent magnetic flux:

$$H = -t_0 \sum_{\langle \mathbf{l}\mathbf{j} \rangle, \sigma} [e^{i\phi_{\mathbf{l}\mathbf{j}}(t)} \tilde{c}_{\mathbf{l},\sigma}^\dagger \tilde{c}_{\mathbf{j},\sigma} + \text{H.c.}] + J \sum_{\langle \mathbf{l}\mathbf{j} \rangle} \mathbf{S}_{\mathbf{l}} \cdot \mathbf{S}_{\mathbf{j}}, \quad (1)$$

where $\tilde{c}_{\mathbf{j},\sigma} = c_{\mathbf{j},\sigma}(1 - n_{\mathbf{j},-\sigma})$ is a projected fermion operator and $\langle \mathbf{l}\mathbf{j} \rangle$ denote nearest neighbors. The constant electric field F is switched on at time $t = 0$ and is measured in units of $[t_0/e_0a]$, where e_0 is the unit charge and a is the lattice distance. We set $t_0 = \hbar = e_0 = a = 1$. For the ladder the charge current operator for $t > 0$ reads

$$\hat{I} = it_0 \sum_{\mathbf{j},\sigma} (e^{-iFt} \tilde{c}_{\mathbf{j}+\hat{x},\sigma}^\dagger \tilde{c}_{\mathbf{j},\sigma} - \text{H.c.}), \quad (2)$$

where F acts along the ladder's leg and $\phi_{\mathbf{l}\mathbf{j}}(t)$ equals $-Ft$ and 0 for hopping in the \hat{x} and \hat{y} direction, respectively.

At this stage it is instructive to recall a simple relation between the current $j(t) = \langle \hat{I}(t) \rangle$ and the total energy $E(t) = \langle H(t) \rangle$ [19], $\dot{E}(t) = FI(t)$, which allows one to calculate the steady component of $j(t)$

$$\bar{j} = \lim_{t \rightarrow \infty} \frac{1}{t} \int_0^t d\tau j(\tau) = \frac{\Delta E(t)}{tF}, \quad (3)$$

where $\Delta E(t) = E(t) - E(0)$.

Ladder.—The real-time response of a ladder with L rungs is studied in the full Hilbert space by means of ED. Applying the Lanczos technique we have determined the initial ground state $|\Psi(t=0)\rangle$ at $\mathbf{p}_0 = (\pi/2, 0)$ [20]. The time evolution of the initial state is calculated by step-wise change of the flux $\phi_{lj}(t)$ in small time increments $\delta t \ll 1$, employing at each step Lanczos basis generating the evolution $|\Psi(t - \delta t)\rangle \rightarrow |\Psi(t)\rangle$ [19,21].

Figure 1(a) demonstrates how the total energy changes in time. One can identify three regimes/limits of F : the adiabatic regime (AR) for $F \rightarrow 0$, the Bloch—oscillations regime (BR) for $F \gg 1$, and the dissipative regime (DR) for intermediate F . In the adiabatic limit, $E(t)$ follows the ground state dispersion $E_0(\mathbf{p})$ with $\mathbf{p} = \mathbf{p}_0 + Ft\hat{x}$. In the ladder $E_0(\mathbf{p})$ is separated from excited states by a finite gap, related to spin gap. The dispersion is a quasiparticle (QP) one; i.e., it follows the behavior of a single carrier with the periodicity $\Delta p_x = 2\pi$. As a result $E(t)$ oscillates with the Bloch frequency $\omega_B = 2\pi/t_B = F$ also in AR. Because of finite gap, qualitatively similar behavior remains even for $|F| > 0$. We expect that the crossover from AR to DR is connected with a transition through the gap resembling the Landau-Zener transition through the Mott-Hubbard gap [5]. Hence, the threshold F should be determined by J .

Figure 1(a) shows that $E(t)$ is monotonic only in DR where $j(t)$ does not change sign. Other regimes (AR, BR) are characterized by strong current oscillations. Figure 1(a)

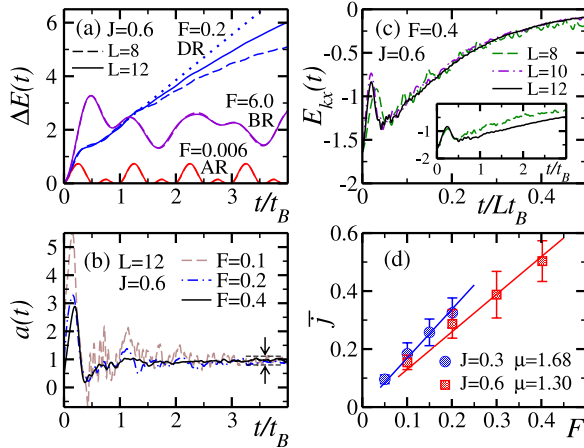


FIG. 1 (color online). Ladder with L rungs: (a) increase of energy $\Delta E(t)$ in different regimes; (b) real-time current $j(t)$ normalized by kinetic energy $a(t) = j(t)/(F|E_{kx}(t)|)$ (note the steady F -independent ratio); (c) kinetic energy E_{kx} vs t/t_B (inset) and t/Lt_B (main); (d) steady current \bar{j} vs F . Dotted line in (a) shows $\Delta E(t)$ estimated from the mobility μ shown in (d) as linear fits $\bar{j} = \mu F$. $J = 0.6$ is used in (a)–(c).

together with Eq. (3) allow one to estimate \bar{j} as a function of the electric field. Clearly \bar{j} is *maximal* in DR; therefore, there exists a corresponding “optimal” F . Substantial differences between the regimes show up also in the kinetic energy related with the movement along the \hat{x} direction, $E_{kx} = \langle H_{kx} \rangle$, where $H_{kx} = -t_0 \sum_{j,\sigma} (e^{-iFt} \tilde{c}_{j+\hat{x},\sigma}^\dagger \tilde{c}_{j,\sigma} + \text{H.c.})$. We have found that $E_{kx}(t)$ oscillates in AR and BR. This quantity is always negative in AR, whereas in BR it takes on negative as well as positive values. Therefore, BR resembles the BO of noninteracting particles in that both $j(t)$ and $E_{kx}(t)$ change sign.

Nonzero \bar{j} in DR implies a steady growth of energy due to the Joule heating (although we are not dealing with well defined thermalization). This effect is limited by the system size since a carrier driven by constant F propagates many times around the ladder with finite L , thus steadily excites the spin background and increases its effective temperature. Figure 1(a) shows that $\Delta E(t)$ deviates considerably between different L at time $t_1 \simeq 2t_B$. As there is a single charge carrier, the quantity $r(t) = \int_0^t d\tau j(\tau) = \Delta E(t)/F$ [see Eq. (3)] can be viewed as a distance traveled by a carrier within the time-interval $(0, t)$. For noninteracting case $\Delta E(t) < 4$ and $r(t) < 4/F$, which is the Stark localization length [22]. Here, we have found that $r(t_1) \sim L$ confirming that the finite-size effects originate from heating of the spin background when carrier repeatedly encircles the ladder.

However, even for $t > t_1$ one can follow the behavior in a controlled way. Previous analysis of 1D system of spinless fermions has shown that heating can be accounted for by a renormalization of the kinetic energy, as a sum rule for the optical conductivity $\sigma(\omega)$ [19]. Results in Fig. 1(b) show that the same reasoning can be applied to the t - J ladder. In particular, the ratio $a(t) = j(t)/(F|E_{kx}(t)|)$ reaches already at short t/t_B nearly a constant value that is independent of F and L . Therefore, the original problem concerning the evaluation of \bar{j} can be reduced to finding $E_{kx}^* = E_{kx}(t \rightarrow \infty)$ in the limit $L \rightarrow \infty$.

A straightforward expectation is that for n -times larger system ($L \rightarrow nL$) it takes n times longer to reach the same average temperature of the spin background. It explains the $E_{kx} \propto E_{kx}(t/L)$ scaling visible for $t > t_1$ in Fig. 1(c). The initial value of E_{kx} in this time domain represents the upper bound on E_{kx}^* when $L \rightarrow \infty$. On the other hand, for $t < t_1$ results for $E_{kx}(t)$ merge without any rescaling of time [see the inset in Fig. 1(c)]. Hence the final value of E_{kx} in the latter time—domain poses the lower bound on E_{kx}^* . These bounds on E_{kx}^* together with the ratio $a(t)$ allow one to extract \bar{j} [see Fig. 1(d)]. Within presented range of F , in the DR nonlinear effects are weak and one can easily estimate the hole mobility: $\mu \sim 1.7$ for $J = 0.3$ and $\mu \sim 1.3$ for $J = 0.6$. However, significant nonlinear effects have to show up for larger fields since \bar{j} is maximal for a finite F . This observation together with the value of μ are the main results for the ladder system.

2D square lattice.—Since in the ground state a single carrier in 2D lattice carries momentum $\mathbf{k}_0 = (\pi/2, \pi/2)$, we set $\phi_{1j}(t) = -Ft/\sqrt{2}$ for the \hat{x} as well as the \hat{y} direction, and $\omega_B = F/\sqrt{2}$. Accordingly, we also define and calculate the modified current $j(t)$, Eq. (2), along the diagonal. We employ an ED method at defined over a limited functional space (EDLFS) which describes properties of a carrier doped into planar ordered AFM [17]. One starts from a translationally invariant state of a carrier in the Néel background $|\phi_0\rangle = c_{\mathbf{k}_0}|\text{Néel}\rangle$. The kinetic part H_k as well as the off-diagonal spin-flip part \tilde{H}_J of the Hamiltonian (1) are applied up to N_h times generating the basis vectors: $\{|\phi_l^{n_h}\rangle\} = [H_k(F=0) + \tilde{H}_J]^{n_h}|\phi_0\rangle$ for $n_h = 0, \dots, N_h$. The ground state $|\Psi(t=0)\rangle$ and its time evolution under electric field are calculated within the limited functional space in the same way as previously for the ladder within the full Hilbert space. The advantage of EDLFS over the standard ED follows from systematic generation of selected states which contain spin excitations in the vicinity of the carrier. It enables investigation of the dynamics of large systems, which are far beyond the reach of ED. Since N_h determines the accessible energies (spin excitations), this quantity poses limits on the maximal propagation time characterized by a steady growth of energy. We set $N_h = 14$ while smaller values of N_h are used to establish the time window, where results are independent of N_h [see inset in Fig. 2(a)].

AR at small $F = 0.1$ is clearly seen from Figs. 2(a) and 2(b) that show $\Delta E(t)$ and $j(t)$ after the field has been switched on at $t = 0$. Both quantities are consistent with the adiabatic propagation along the QP band with a period $t_p = t_B/2$, consistent with the AFM long range order. In the DR the carrier starts to move due to the constant field, it emits magnons and, consequently, after propagation

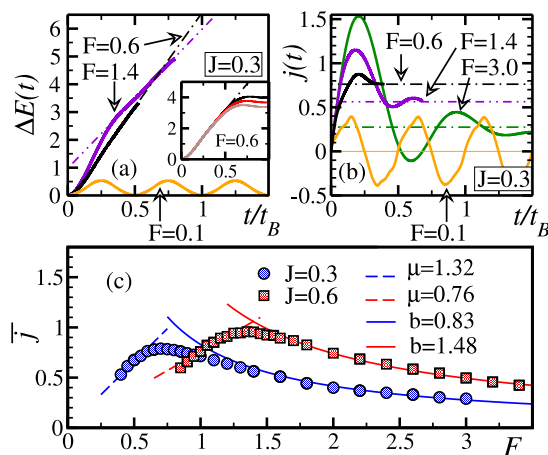


FIG. 2 (color online). 2D lattice: (a) increase of energy $\Delta E(t)$ for $J = 0.3$, various F (main) and $N_h = 12, 13, 14$ (inset); (b) real-time current $j(t)$, \bar{j} from Eq. (3) (dotted-dashed lines); (c) steady current \bar{j} vs F fitted by $\bar{j} = \mu F$ (dashed lines) and $\bar{j} = b/F$ (solid lines) in PDR and NDR regimes, respectively.

through the transient regime $t/t_B \ll 1$, it develops a finite average velocity as seen for $F = 0.6$ and 1.4 . DR is characterized by a constant current and a linear increase of the total energy of the system. To calculate the current we make use of Eq. (3) where the linear increase of $\Delta E(t)$ provides the value of \bar{j} . Indeed, linear dotted-dashed fits in Fig. 2(a) indicate that the system has already reached the quasi stationary state. We plot the extracted values of \bar{j} as dotted-dashed horizontal lines in Fig. 2(b). Similar approach has recently been applied to the problem of a driven Holstein polaron [18]. At large field, $F \gtrsim 3$, $j(t)$ is consistent with a damped BO with $t_p \lesssim t_B$, signaling the onset of BR.

Figure 2(c) displays \bar{j} - F characteristics in DR for $J = 0.3$ and $J = 0.6$. Each point has been calculated from Eq. (3) and then compared with $j(t)$, as demonstrated in Figs. 2(a) and 2(b). The most remarkable property is a peak at F_0 dividing DR into two subregimes, i.e., the regime of positive differential resistivity (PDR) for $F < F_0$ and the regime of negative differential resistivity (NDR) for $F > F_0$. The value of the crossover field F_0 scales with the exchange energy J . From curves in Fig. 2(c) we find $F_0 \approx 2.3J$. This is consistent with an intuitive expectation that the onset of the NDR regime emerges when the energy gained by a single hop exceeds the maximal energy of one-magnon excitation. Consequently, the real-space propagation of a carrier exhibits qualitatively different behavior in both regimes. This is illustrated in Fig. 3 which displays spin deformation function $C(\mathbf{r})$ around the carrier at different times. We define $C(\mathbf{r}) = \sum_i \langle n_i | S_{i+r}^{z, \text{Néel}} - S_{i+r}^z | \rangle$ with $S_j^{z, \text{Néel}} = \pm \frac{1}{2}$. In the PDR regime and for $F = 0.6$ spin excitations predominantly emerge behind the traveling carrier indicating that the average charge velocity \bar{v}_c is larger than magnon velocity $v_s = \sqrt{2}J$, i.e. $\bar{v}_c = \bar{j} > v_s$ (see the upper panel of Fig. 3). A more complex pattern characterizes the NDR regime

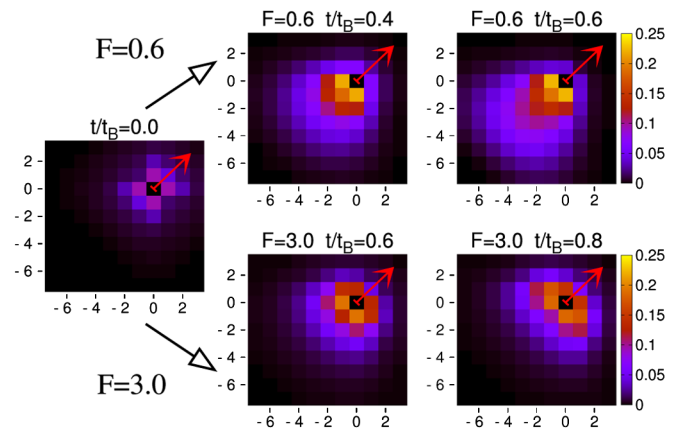


FIG. 3 (color online). 2D lattice with $J = 0.3$. Snapshots of the spin deformation $C(\mathbf{r})$ in the vicinity of hole [placed at $(0,0)$], taken at different times t/t_B . Solid arrows indicate direction of the electric field.

where at $F = 3$, $\bar{v}_c < v_s$ (lower panel of Fig. 3) and enhanced spin excitations develop also in front of the carrier. Moreover, $C(\mathbf{r})$ displays a distinct transverse orientation with respect to the field direction. This signals an increased transverse and longitudinal carrier oscillation that serves to release the excess energy to the unperturbed spin background.

In the PDR regime (dashed lines in Fig. 2(c)) linear fits of the current increase provide an estimate for the carrier mobility, which yields $\mu \sim 1.3$ for $J = 0.3$ and $\mu \sim 0.8$ for $J = 0.6$. These values are in agreement with ED calculations using the linear—response theory [23] and indicate that carrier mobility increases with growing correlations. In the NDR regime a scaling $\bar{j} \sim 1/F$ is found, Fig. 2(c). This is consistent with incoherent hopping between Stark states appropriate for dispersive boson excitations [24], in contrast to coherent hopping in the case of dispersionless phonons leading to $\bar{j} \propto 1/\sqrt{F}$ [18].

Discussion.—At small F the ladder and the 2D system exhibit adiabatic propagation with $\bar{j} = 0$. The validity of AR is closely connected with the stability of the lowest QP band. While this is more evident for the ladder (due to a gap), the gapless (acoustic) magnons in 2D lattice require more care. Nevertheless, our results show that the condition for Cherenkov radiation of magnons $v(k) > v_s = \sqrt{2}J$ is for $J \geq 0.3$ never fulfilled. In part, because the QP bandwidth is limited by J and not by t . For $J = 0.3$ we obtain maximal charge velocity $v_{\max} = 1.36J$ while for $J = 0.6$, $v_{\max} = 1.10J$. Moreover, the QP weight remains finite throughout the whole Brillouin zone [17,25].

With increasing F both systems enter DR where the quasistationary current is proportional to F , leading to well defined mobility being even quantitatively close for both cases. The mechanism of dissipation is clearly the emission of spin excitations. Still the dissipation is due to topological difference (in particular due to the possibility of spin perturbation transverse to the direction of the carrier propagation) more efficient within the 2D lattice leading to stronger damping of the BO and finite $\bar{j} \propto 1/F$. Consequently, quasistationary current on the square lattice occurs up to much larger F than in the ladder where in the same regime strong BO with $\bar{j} \sim 0$ prevail.

Surprisingly, the undoped [11] and lightly doped MI show the same sequence of the field—regimes: \bar{j} is zero or exponentially small for sufficiently weak F (AR in the present case); for larger F the linear \bar{j} - F dependence is restored (DR); finally, for very large F the response is dominated by the BO (BR). However, in doped and undoped MI these regimes occur at exceedingly different fields. In particular, the DMFT studies of the strong- U limit [11] reveal that the threshold field for the dielectric breakdown of undoped MI is $F_{\text{th}} \gg 1$, which is an order of magnitude above the field discussed here.

L. V. and J. B. acknowledge stimulating discussions with T. Tohyama and O. P. Sushkov. This work has been

supported by the Program P1-0044 of the Slovenian Research Agency (ARRS) and REIMEI project, JAEA, Japan. M. M. acknowledges support from MNiSW Grant N202 052940.

-
- [1] L. Perfetti *et al.*, *Phys. Rev. Lett.* **97**, 067402 (2006); A. L. Cavalieri *et al.*, *Nature (London)* **449**, 1029 (2007); A. Pashkin *et al.*, *Phys. Rev. Lett.* **105**, 067001 (2010).
 - [2] L. M. K. Vandersypen *et al.*, *Appl. Phys. Lett.* **85**, 4394 (2004); M. Grobis *et al.*, *Phys. Rev. Lett.* **100**, 246601 (2008).
 - [3] S. Trotzky *et al.*, *Science* **319**, 295 (2008); U. Schneider *et al.*, *Science* **322**, 1520 (2008).
 - [4] P. Barmettler, *New J. Phys.* **12**, 055017 (2010).
 - [5] T. Oka, R. Arita, and H. Aoki, *Phys. Rev. Lett.* **91**, 066406 (2003).
 - [6] H. Fehske *et al.*, *Phys. Lett. A* **373**, 2182 (2009).
 - [7] S. R. White and A. E. Feiguin, *Phys. Rev. Lett.* **93**, 076401 (2004); J. Eckel *et al.*, *New J. Phys.* **12**, 043042 (2010).
 - [8] J. K. Freericks, V. M. Turkowski, and V. Zlatic, *Phys. Rev. Lett.* **97**, 266408 (2006); M. Eckstein *et al.*, *Eur. Phys. J. Special Topics* **180**, 217 (2010).
 - [9] Y. Taguchi, T. Matsumoto, and Y. Tokura, *Phys. Rev. B* **62**, 7015 (2000).
 - [10] T. Oka and H. Aoki, *Phys. Rev. Lett.* **95**, 137601 (2005); A. Takahashi, H. Itoh, and M. Aihara, *Phys. Rev. B* **77**, 205105 (2008);
 - [11] M. Eckstein, T. Oka, and P. Werner, *Phys. Rev. Lett.* **105**, 146404 (2010).
 - [12] S. Weiss *et al.*, *Phys. Rev. B* **77**, 195316 (2008); E. Boulat, H. Saleur, and P. Schmitteckert, *Phys. Rev. Lett.* **101**, 140601 (2008); F. Heidrich-Meisner, A. E. Feiguin, and E. Dagotto, *Phys. Rev. B* **79**, 235336 (2009); C. Karrasch *et al.*, *Europhys. Lett.* **90**, 30003 (2010).
 - [13] F. Heidrich-Meisner *et al.*, *Phys. Rev. B* **82**, 205110 (2010).
 - [14] Y. Kanamori, H. Matsueda, and S. Ishihara, *Phys. Rev. Lett.* **103**, 267401 (2009); H. Matsueda, T. Tohyama, and S. Maekawa, arXiv:1005.1690.
 - [15] K. A. Al-Hassanieh *et al.*, *Phys. Rev. Lett.* **100**, 166403 (2008); W. Koshibae, N. Furukawa, and N. Nagaosa, *Phys. Rev. Lett.* **103**, 266402 (2009).
 - [16] E. Dagotto, *Rev. Mod. Phys.* **66**, 763 (1994).
 - [17] J. Bonca, S. Maekawa, and T. Tohyama, *Phys. Rev. B* **76**, 035121 (2007); L. Vidmar *et al.*, *Phys. Rev. Lett.* **103**, 186401 (2009).
 - [18] L. Vidmar *et al.*, *Phys. Rev. B* **83**, 134301 (2011).
 - [19] M. Mierzejewski and P. Prelovsek, *Phys. Rev. Lett.* **105**, 186405 (2010).
 - [20] M. Greiter, *Phys. Rev. B* **65**, 134443 (2002).
 - [21] T. J. Park and J. C. Light, *J. Chem. Phys.* **85**, 5870 (1986).
 - [22] A. R. Kolovsky, *Phys. Rev. Lett.* **101**, 190602 (2008).
 - [23] J. Jaklic and P. Prelovsek, *Phys. Rev. B* **52**, 6903 (1995).
 - [24] D. Emin and C. F. Hart, *Phys. Rev. B* **36**, 2530 (1987).
 - [25] P. W. Leung and R. J. Gooding, *Phys. Rev. B* **52**, R15711 (1995).